

# Mechanism of the Germyl Wright–West Anionic Migration. *Ab Initio* Theoretical Study of Counterion Effects and Comparison with the Analogous Silyl and Methyl (Wittig) Rearrangements

Paola Antoniotti and Glauco Tonachini\*

Dipartimento di Chimica Generale ed Organica Applicata, Università di Torino,  
Corso Massimo D'Azeglio, 48 I-10125 Torino, Italy

Received May 27, 1999

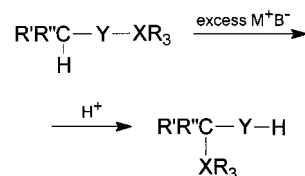
The mechanism of the [1,2] germyl rearrangement in the  $(\text{H}_2\text{COGeH}_3)\text{Li}$  model system is studied and compared with the results previously obtained for (1) the corresponding free anion model and (2) the two formally similar silyl and methyl migrations. The mechanism of the germanium rearrangement is found to diverge from both of these. The *nondissociative rearrangement pathway* is a one-step [1,2] Ge shift and does not involve a cyclic intermediate, in contrast with the two-step mechanism of the silicon migration. A transition structure with pentacoordinate Ge, similar to the cyclic intermediate found for Si, is located ca. 17 kcal mol<sup>-1</sup> above the initial lithiated carbanion. The energy shoulder previously found in the free anion Ge system, in correspondence of such a geometry, completely disappears when Li<sup>+</sup> interacts with the anionic system. As the energy barrier is raised with respect to the anion, where it was only 2 kcal mol<sup>-1</sup> high, the transition structure becomes later, in a geometrical sense. Concurrently, the exoergicity ( $\Delta E = -24$  kcal mol<sup>-1</sup>) is reduced to some extent with respect to the free anion ( $\Delta E = -30$  kcal mol<sup>-1</sup>). A *dissociation/reassociation pathway* is then explored, which leads, via O–Ge bond cleavage, to a rather stable complex between the two  $\text{H}_2\text{CO}$  and  $\text{LiGeH}_3$  moieties ( $-10$  kcal mol<sup>-1</sup>). However, similarly to silicon, the energy barrier for the dissociative process (ca. 30 kcal mol<sup>-1</sup>) is higher (by 13 kcal mol<sup>-1</sup>) than that for direct germyl migration, which is as a consequence the preferred pathway. Also in the free anion the dissociation pathway was required to overcome an energy barrier higher than that for direct [1,2] shift by 8 kcal mol<sup>-1</sup>. A similar situation had been found for silicon too. This result contrasts the description recently obtained for the Wittig carbon rearrangement that shows a sharp preference for a dissociation/reassociation mechanism.

## Introduction

The transformation of silyl and germyl ethers (or sulfides) into their isomeric alcohols (or thiols) was investigated years ago by Wright and West.<sup>1</sup> These reactions take place, in the presence of excess strong base, through electrophilic rearrangements of different silyl and germyl groups on anionic carbon–oxygen or carbon–sulfur skeletons (Scheme 1). Therefore, they are the silicon and germanium analogues of the famous Wittig rearrangement,<sup>2</sup> in which the carbon-centered migrating moiety is an alkyl, aryl, or allyl group.

The electrophilic migration reactions belonging to this family span, as regards the X-centered migrating group, three rows of the periodic table. Although they all are formally similar, it is legitimate to question if resemblance is a façade. The purpose of a series of theoretical mechanistic studies, carried out in the last years in this laboratory, has been that of offering a contribution to

## Scheme 1



(X = C, Si, Ge; Y = O, S)

understanding the real concern of this likeness. The theoretical study of the Ge Wright–West reaction has already been undertaken for the free anion,<sup>3</sup> by studying the germyl migration from oxygen to carbon in the simple  $(\text{H}_2\text{COGeH}_3)^-$  system. This study has indicated that the direct germyl migration takes place as a one-step process. The analogous silicon system and its lithiated counterpart had been investigated in two foregoing papers,<sup>4</sup> while the Wittig migration has been ana-

\* Corresponding author. Fax: 39-011-6707642. E-mail: tonachini@silver.ch.unito.it.

(1) (a) Wright, A.; West, R. *J. Am. Chem. Soc.* **1974**, *96*, 3214–3222. (b) Wright, A.; West, R. *J. Am. Chem. Soc.* **1974**, *96*, 3222–3227. (c) Wright, A.; West, R. *J. Am. Chem. Soc.* **1974**, *96*, 3227–3232.

(2) (a) Wittig, G.; Lohmann, L. *Ann.* **1942**, *550*, 260–268. (b) Wittig, G. *Angew. Chem.* **1954**, *66*, 10–17.

(3) (a) Antoniotti, P.; Tonachini, G. *Organometallics* **1996**, *15*, 1307–1314. (b) Antoniotti, P.; Canepa, C.; Tonachini, G. *Trends Org. Chem.* **1995**, *5*, 189–201.

(4) (a) Antoniotti, P.; Tonachini, G. *J. Org. Chem.* **1993**, *58*, 3622–3632. (b) Antoniotti, P.; Canepa, C.; Tonachini, G. *J. Org. Chem.* **1994**, *59*, 3952–3959.

lyzed in detail recently.<sup>5</sup> The results obtained so far indicate that different reaction mechanisms are operative for the three H<sub>2</sub>COXH<sub>3</sub> anionic systems. The homolytic dissociation followed by reassociation found for X = C is contrasted by a two-step direct (nondissociative) migration, passing through a cyclic intermediate, observed when X = Si. However, these results are incomplete, because the Ge system has been investigated only as a free anion, while the C and Si systems were studied also in their lithiated forms, to provide two extreme pictures of no interaction and tight interaction with the counterion. Therefore, in an effort to provide a more convincing and complete description, the behavior of the (H<sub>2</sub>COGeH<sub>3</sub>)Li system is explored in the present study. A conceivable competition between the direct [1,2] shift and a dissociative/reassociative process is considered. The latter would involve cleavage of the Ge–O bond and possible formation of an intermediate complex. In the case of the germanium free anion and in the case of the silicon system this pathway was found not to be competitive with the direct shift.

## Methods

The study of the rearrangement reaction was performed by determining on the energy hypersurface the critical points relevant to stable and transition structures. This was accomplished by way of complete gradient optimization<sup>6</sup> of the geometrical parameters at the second-order of the Møller–Plesset perturbation theory.<sup>7</sup> MP2 optimizations were carried out with the split-valence shell spd basis set by Huzinaga and co-workers, enriched with diffuse p functions and d polarization functions on all non-hydrogen atoms. This computational level will be denoted as MP2/[552/331/2/31] in the following, thus indicating how the spd basis functions are grouped for Ge/C,O/H/Li, respectively.<sup>8</sup> The O–Ge bond cleavage transition structure from the initial carbanion was redetermined by complete active space multiconfiguration self-consistent-field<sup>9</sup> optimizations. In these optimizations the diffuse functions were eliminated because they generated serious convergence problems. These CAS-MCSCF/[542/321/2/21] calculations involve four active orbitals and four electrons in the active space.<sup>10</sup> Then, an intrinsic reaction coordinate (IRC) analysis<sup>11</sup> was carried out in the vicinities of the dissociation transition structure, to unambiguously define the geometrical features

of the relevant pathway. In addition, a whole series of CAS-MCSCF/[542/321/2/21] constrained geometry optimizations was performed, with the aim of defining the nature of the wave function changes along a more extended portion of the dissociation pathway. In the figures of the following section the reported interatomic distances are in ångströms, and angles in degrees; dihedral angles are reported in parentheses. The critical points were characterized as minima or first-order saddle points, corresponding to a transition structure (TS), through diagonalization of the analytically calculated Hessian matrix (vibrational frequencies calculation). Dynamic correlation effects were then taken care of by means of the coupled cluster method.<sup>12</sup> The Huzinaga basis set was compared with the Pople 6-311+G(d) basis set,<sup>13</sup> by executing a test on the dissociation barrier. This provided very similar CAS-MCSCF/[542/321/2/21] and 6-311+G(d) TS geometries. Subsequent CCSD(T)/[552/331/2/31] and 6-311+G(d) single-point energy calculations provided in turn close barrier estimates (the latter basis set supplies lower energies). Thus, it was decided to unify the two parts of the study by defining more homogeneous energy profiles for both the nondissociative and dissociative processes: to this purpose, the MP2 and CAS-MCSCF geometries were used to recompute the relative energies at the CCSD(T)/6-311+G(d) level. The dissociation profile was better defined by a series of additional points, obtained by constrained optimizations (see the following section for details). The evolution of the electron distribution during the germyl dissociation process was examined by computing NAO group charges, within a natural bond orbital analysis.<sup>14</sup> The GAUSS-IAN94 system of programs<sup>15</sup> was used for all calculations.

## Results and Discussion

Germylloxymethylithium is the initial “reactant” (Figure 1a). It presents three conformational minima.

(10) (a) In these computations, the active space chosen consists of four orbitals populated with four electrons. The orbitals were initially defined, to make an unambiguous choice, for three separated fragments: formaldehyde, germyl, and lithium. Two active orbitals belong to the formaldehyde-like fragment, the quasi- $\pi$  and quasi- $\pi^*$  couple; one is a  $\sigma$  orbital localized on the methyl group, and one is an empty 2s orbital of Li<sup>+</sup>. In this respect orbital optimization defines the more appropriate admixture of lithium empty valence sp orbitals for each structure. A complete CI in this active space corresponds to 20 configurations. (b) The two configurations with highest coefficients along the dissociation pathway can be described as follows. One has double occupancy of two orbitals: (1) that made up by an in-phase combination of the quasi- $\pi_{CO}$  and a  $\sigma_{GeH_3}$  orbital directed toward oxygen; (2) that defined by an in-phase combination of the quasi- $\pi^*_{CO}$  and the same  $\sigma_{GeH_3}$ . The second configuration in order of importance has double occupancy of the orbital (1) just described and double occupancy of an out-of-phase combination of the quasi- $\pi^*_{CO}$  with the same  $\sigma_{GeH_3}$ .

(11) (a) Gonzalez, C.; Schlegel, H. B.; *J. Chem. Phys.* **1989**, *90*, 2154–2161. (b) Gonzalez, C.; Schlegel, H. B.; *J. Phys. Chem.* **1990**, *94*, 5523–5527.

(12) (a) Coester, F.; Kümmel, H. *Nucl. Phys.* **1960**, *17*, 477. (b) Cizek, J. *J. Chem. Phys.* **1966**, *45*, 4256–4266. (c) Paldus, J.; Cizek, J.; Shavitt, I. *Phys. Rev. A* **1972**, *5*, 50–67. (d) Pople, J. A.; Krishnan, R.; Schlegel, H. B.; Binkley, J. S. *Int. J. Quantum Chem.* **1978**, *14*, 545–560. (e) Bartlett, R. J.; Purvis, G. D. *Int. J. Quantum Chem.* **1978**, *14*, 561–581. (f) Cizek, J.; Paldus, J. *Phys. Scr.* **1980**, *21*, 251–254. (g) Bartlett, R. J. *Annu. Rev. Phys. Chem.* **1981**, *32*, 359–401. (h) Purvis, G. D.; Bartlett, R. J. *J. Chem. Phys.* **1982**, *76*, 1910–1918. (i) Scuseria, G. E.; Janssen, C. L.; Schaefer, H. F., III *J. Chem. Phys.* **1988**, *89*, 7382–7387. (j) Scuseria, G. E.; Schaefer, H. F., III *J. Chem. Phys.* **1989**, *90*, 3700–3703.

(13) (a) Binkley, J. S.; Pople, J. A.; Hehre, W. J. *J. Am. Chem. Soc.* **1980**, *102*, 939–947. (b) Clark, T.; Chandrasekhar, J.; Schleyer, P. v. R. *J. Comput. Chem.* **1983**, *4*, 294. (c) Hariharan, P. C.; Pople, J. A. *Theor. Chim. Acta* **1973**, *28*, 213–222. (d) Frisch, M. J.; Pople, J. A.; Binkley, J. S. *J. Chem. Phys.* **1984**, *80*, 3265–3269. The basis set for germanium corresponding to the “6-311G” keyword is actually a (15s11p6d) contracted to [8s7p3d], without any sharing of the exponential coefficients.

(14) Reed, A. E.; Weinstock, R. B.; Weinhold, F. *J. Chem. Phys.* **1985**, *83*, 735–746. Reed, A. E.; Weinhold, F. *J. Chem. Phys.* **1983**, *78*, 4066–4073. Foster, J. P.; Weinhold, F. *J. Am. Chem. Soc.* **1980**, *102*, 7211–7218.

(5) Antonietti, P.; Tonachini, G. *J. Org. Chem.* **1998**, *63*, 9756–9762.

(6) (a) Schlegel, H. B. In *Computational Theoretical Organic Chemistry*; Csizsmadia, I. G., Daudel, R., Eds.; Reidel Publ. Co.: Dordrecht, 1981; p 129. (b) Schlegel, H. B. *J. Chem. Phys.* **1982**, *77*, 3676–3681. (c) Schlegel, H. B.; Binkley, J. S.; Pople, J. A. *J. Chem. Phys.* **1984**, *80*, 1976–1981. (d) Schlegel, H. B. *J. Comput. Chem.* **1982**, *3*, 214.

(7) (a) Møller, C.; Plesset, M. S. *Phys. Rev.* **1934**, *46*, 618. (b) Binkley, J. S.; Pople, J. A. *Int. J. Quantum Chem.* **1975**, *9*, 229–236. (c) Pople, J. A.; Binkley, J. S.; Seeger, R. *Int. J. Quantum Chem. Symp.* **1976**, *10*, 1–19. (d) Krishnan, R.; Pople, J. A. *Int. J. Quantum Chem. Symp.* **1980**, *14*, 91.

(8) Huzinaga, S.; Andzelm, J.; Klobukowski, M.; Radzio-Andzelm, E.; Sakai, Y.; Tatewaki, H. *Gaussian Basis Sets for Molecular Calculations*. In *Physical Sciences Data 16*; Elsevier: Amsterdam, 1984. For further details, see ref 3, footnote 11. The lithium basis set consists of 7 s primitive Gaussians (the last one a diffuse set with exponent 0.02529) grouped following a 421 scheme (3 resulting s Gaussians); a single p Gaussian is also added. This 3s1p basis is denoted as [31] and is reduced to [21] in the MCSCF calculations, in which the diffuse functions have been dropped. Similarly, the Ge [552]/C,O [331] basis sets of the MP2 and CCSD(T) calculations reduce to [542] and [321] in the MCSCF calculations.

(9) (a) Hegarty, D.; Robb, M. A. *Mol. Phys.* **1979**, *38*, 1795–1812. (b) Robb, M. A.; Eade, R. H. A. *NATO Adv. Study Inst. Ser.* **1981**, *C67*, 21–54. See also, for a discussion of the method: Roos, B. *The Complete Active Space Self-Consistent Field Method and its Applications in Electronic Structure Calculations*. In *Ab Initio Methods in Quantum Chemistry-II*; Lawley, K. P. Ed.; J. Wiley & Sons Ltd.: New York, 1987.

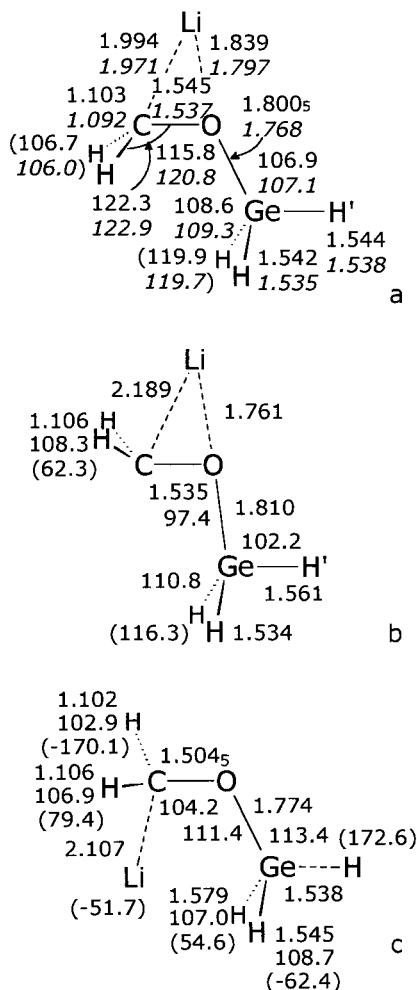


**Figure 1.** Germyloxymethyl lithium: (a) the more stable “W” minimum ( $C_s$ ), with Li and Ge in an antiperiplanar conformation; (b) “Y” minimum ( $C_s$ ), with antiperiplanar Li and Ge; (c) gauche minimum ( $C_1$ ). Dihedral angles (reported in parentheses) are HCOLi and HGeOH’ for the  $C_s$  structures; HCOGe, LICOGel, and HGeOC for the  $C_1$  structure. Regular typeface: MP2 values. Italic (W minimum only): CAS-MCSCF values.

In **1a** the cation is involved in a bridging interaction with both carbon and oxygen; the C–Li bond is therefore antiperiplanar with respect to the O–Ge bond. This conformation is the same found for the free anion. It will be labeled for convenience as W, from the position of germanium relative to the two methylenic hydrogens in a Newman projection. Another conformational minimum (labeled as Y), in which lithium is still anti to germanium, has the methylenic group pyramidalized in the opposite direction with respect to the O–Ge bond (Figure 1b). This secondary minimum is rather high in energy with respect to **1a** (Table 1). In **1b** the LiC bond is longer than in **1a**, and the LiO bond is shorter, but lithium is still in a bridging position between carbon and oxygen. The inversion on carbon with respect to **1a**

shifts a large share of the electron density close to germanium, and this concentration exerts some attraction onto it. In fact, the COGe angle undergoes a significant change with respect to **1a**, being smaller by 18°. The stability of structure **1a** shows, as a consequence, some dependence on the extension of the lithium basis set, whose outer (empty) functions are rather extended and provide some diffusion of the electron density. Limiting the basis flexibility results in reducing the role these outer functions play in stabilizing a structure as **1b**. In fact, if they are eliminated, germanium tends to further move toward carbon, where the electron density is now more concentrated than in the presence of a full basis on  $\text{Li}^+$ . The existence of a well-defined minimum on the energy surface is a rather delicate question of balancing the basis set. The question seems more of a computational than chemical nature. In any case, the chemical importance of this kind of structure is very limited, as will be discussed presently. On one hand, its geometry and its relatively high energy put it close to the transition structure for direct migration; on the other hand, the system has to overcome the related energy barrier anyway. A third stable structure, obtained by rotating the whole  $\text{CH}_2\text{Li}$  group, has lithium gauche to Ge (Figure 1c). Also this secondary minimum is higher in energy than **1a**, but is more stable than **1b** by ca. 5 kcal  $\text{mol}^{-1}$  (Table 1).

In Figure 2 three transition structures (TS) connecting these minima are displayed. One of them (**2a**) corresponds to  $\text{CH}_2$  inversion and connects the W and Y minima ( $\nu_1 = 621.8i \text{ cm}^{-1}$ ). Some important geometrical parameters (e.g., LiC, LiO, GeOC) have proceeded in the TS to about 70% of their total change and make the TS appear to be closer to the Y conformer, consistent with the energy difference between the two minima (however, a linear change in all parameters it is not to be expected: see for instance the CO bond). The second TS (**2b**) could again lead from **1a** to **1b** through a rotation of the  $\text{CH}_2$  group ( $\nu_1 = 389.1i \text{ cm}^{-1}$ ), but is located rather high in energy (Table 1). A third TS (**2c**) relates the W and gauche minima ( $\nu_1 = 109.0i \text{ cm}^{-1}$ ). The transition vector is dominated by the angular parameters of the rotating  $\text{CH}_2\text{Li}$  group.

**The Nondissociative Migration Pathway.** The gas-phase energy profile for a direct migration of the germyl group from oxygen to carbon has first been defined. Figure 3a displays the structure corresponding to a first-order saddle point for the intramolecular migration of the germyl group ( $\nu_1 = 145.3i \text{ cm}^{-1}$ ). As germanium moves toward the carbon atom, lithium leaves carbon and begins a rotation around the oxygen atom (clockwise in Figure 3a). Its interaction with oxygen gets stronger, as witnessed by the shorter distance. The transition vector is dominated by the motion of the germyl group almost parallel to the CO bond (0.71 coefficient for the COGe angle), coupled with the change in the OGe bond length (−0.33 coefficient); smaller contributions, on the order of 0.25, come from the HGeO angles and relevant dihedral angles. A backward IRC shows that this TS is directly connected to the secondary minimum **1b** (Y). This is however a datum of limited significance, due to the dubious importance of this high-energy structure, whose pres-

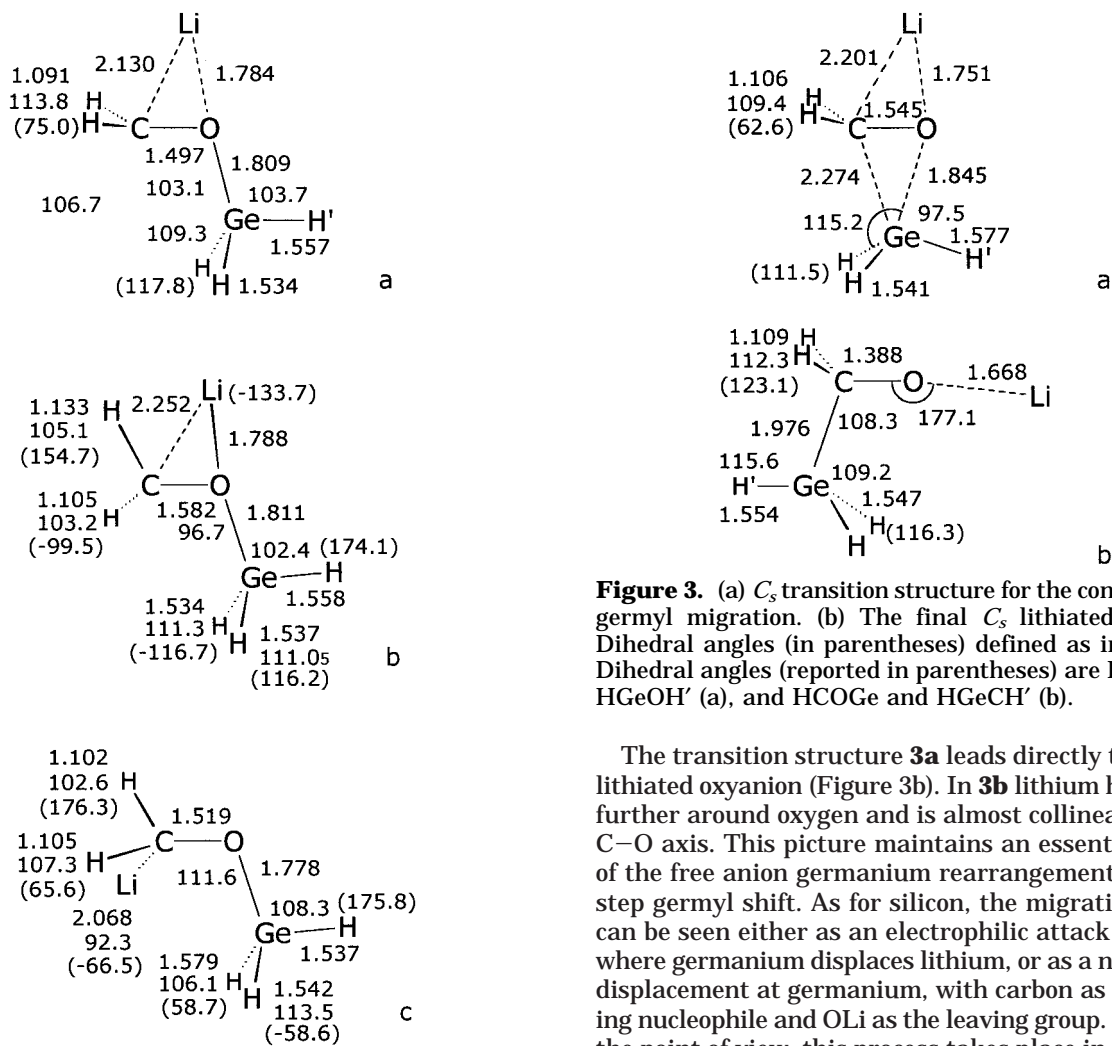
(15) Frisch, M. J.; Trucks, G. W.; Schlegel, H. B.; Gill, P. M. W.; Johnson, B. G.; Robb, M. A.; Cheeseman, J. R.; Keith, T. A.; Petersson, G. A.; Montgomery, J. A.; Raghavachari, K.; Al-Laham, M. A.; Zakrzewski, V. G.; Ortiz, J. W.; Foresman, J. B.; Cioslowski, J.; Stefanov, B. B.; Nanayakkara, A.; Challacombe, M.; Peng, C. Y.; Ayala, P. Y.; Chen, W.; Wong, M. W.; Andres, J. L.; Replogle, E. S.; Gomperts, R.; Martin, R. L.; Fox, D. J.; Binkley, J. S.; Defrees, D. J.; Baker, J.; Stewart, J. P.; Head-Gordon, M.; Gonzalez, C.; Pople, J. A. *GAUSSIAN94*; Gaussian, Inc.: Pittsburgh, PA, 1995.



Table 1. Total<sup>a</sup> and Relative<sup>b</sup> Energies of the Critical Points

structure ( <i>Li to Ge</i> relation)		CCSD(T)/6-311+G(d) <sup>c</sup>		MP2/[552/331/2/3]	
		<i>E</i>	$\Delta E$	<i>E</i>	$\Delta E$
"W" reactant (anti)	<b>1a</b>	-2198.886768	0.0	-2196.784944	0.0
"Y" reactant (anti)	<b>1b</b>	-2198.860983	16.2	-2196.758912	16.3
reactant (gauche)	<b>1c</b>	-2198.868588	11.4	-2196.769131	9.9
TS (from <b>1a</b> to <b>1b</b> , CH <sub>2</sub> inv.)	<b>2a</b>	-2198.858860	17.5	-2196.757807	17.0
TS (from <b>1a</b> to <b>1b</b> , CH <sub>2</sub> rot.)	<b>2b</b>	-2198.845792	25.7	-2196.740542	27.9
TS (from <b>1a</b> to <b>1c</b> , CH <sub>2</sub> Li rot.)	<b>2c</b>	-2198.869105	11.1	-2196.768906	10.1
[1,2] migration TS	<b>3a</b>	-2198.860212	16.7	-2196.758357	16.7
oxyanionic product	<b>3b</b>	-2198.924881	-23.9	-2196.823600	-24.3
dissociation TS <sup>d</sup>	<b>4a</b>	-	-	-2196.737390	29.8
dissociation TS	<b>4b</b>	-2198.826100	38.1	-2196.714920	43.9
electrostatic complex	<b>4c</b>	-2198.902820	-10.1	-2196.799102	-8.9

<sup>a</sup> Hartrees. <sup>b</sup> kcal mol<sup>-1</sup>. <sup>c</sup> Computed at the MP2/[552/331/2] geometries of the critical points. <sup>d</sup> The analysis of this dissociation pathway has been pursued in more detail at the CAS-MCSCF level of theory (see Table 2).



**Figure 3.** (a) C<sub>s</sub> transition structure for the concerted [1,2] germyl migration. (b) The final C<sub>s</sub> lithiated oxyanion. Dihedral angles (in parentheses) defined as in Figure 1. Dihedral angles (reported in parentheses) are HCOLi and HGeOH' (a), and HCOGe and HGeCH' (b).

The transition structure **3a** leads directly to the final lithiated oxyanion (Figure 3b). In **3b** lithium has rotated further around oxygen and is almost collinear with the C–O axis. This picture maintains an essential feature of the free anion germanium rearrangement,<sup>3</sup> the one-step germyl shift. As for silicon, the migration process can be seen either as an electrophilic attack at carbon, where germanium displaces lithium, or as a nucleophilic displacement at germanium, with carbon as the incoming nucleophile and OLi as the leaving group. Whichever the point of view, this process takes place in a different way with respect to the analogous intramolecular silyl [1,2] shift, which proceeds through a cyclic pentacoordinate-Si intermediate.

The energy barrier referred to **1a** is significantly raised with respect to the free anion case: the 17 kcal mol<sup>-1</sup> energy barrier relevant to **3a** can be compared with the 2 kcal mol<sup>-1</sup> of the CH<sub>2</sub> rotational pathway or with the 7 kcal mol<sup>-1</sup> relevant to the CH<sub>2</sub> inversion TS. The counterion evidently stabilizes the initial carbanion more than the TS, possibly due to a redistribution of the electron density toward the germyl group, bringing about some charge delocalization. The exoergicity is reduced to -24 kcal mol<sup>-1</sup> with respect to the -32 kcal

ence as a well-defined energy minimum is moreover bound to a delicate balance of the Li<sup>+</sup> basis set extension. The main consideration is that, whichever is the case, the direct migration pathway has to pass the energy barrier in correspondence to TS **3a**.

$\text{mol}^{-1}$  computed for the free anion. Lithium appears to be more effective in stabilizing a negative charge largely localized on carbon, rather than on the more electronegative oxygen.

Up to this point, the results obtained for the direct [1,2] migration pathway in a situation of tight anion–cation interaction are the following. In contrast with the Si [1,2] shift, the present calculations describe a one-step process, in which the C–Ge bond is formed concertedly with the cleavage of the O–Ge bond. Therefore, no cyclic intermediate with pentacoordinate germanium is involved; a geometry of this kind corresponds to a transition structure. If the overall migration process is less exoergic than in the free anion system by ca. 8 kcal  $\text{mol}^{-1}$ , the energy barrier is concurrently raised by ca. 15 kcal  $\text{mol}^{-1}$ . The barrier of 17 kcal  $\text{mol}^{-1}$  is close to that of silicon (15 kcal  $\text{mol}^{-1}$ ), while the exoergicity,  $-24$  kcal  $\text{mol}^{-1}$ , is significantly larger (Si:  $-13$  kcal  $\text{mol}^{-1}$ ).

**The Dissociative Process.** The reacting system can also dissociate into two fragments, by cleavage of the O–Ge bond. If this is followed by reassociation through formation of a new C–Ge bond, the same product **3b** of the nondissociative migration is obtained. In the silicon migration this kind of pathway was found not to be competitive with the direct shift.<sup>4</sup> By contrast, a recent study of the Wittig rearrangement in a similar system provides the indication that a dissociation/reassociation process corresponds to the preferred pathway.<sup>5</sup>

The heterolytic dissociation limit (formaldehyde and germyllithium) is the lowest one, 8 kcal  $\text{mol}^{-1}$  above **1a** at the CCSD(T) level, while the homolytic (formaldehyde radical anion associated to a lithium cation and germyl radical) is higher in energy by more than 36 kcal  $\text{mol}^{-1}$ . However, the reacting system could dissociate and then reassociate while avoiding the attainment of a dissociation limit. In fact, if germyl were able to dissociate while interacting with  $\text{Li}^+$ , then the resulting  $\text{H}_2\text{CO}$  and  $\text{LiGeH}_3$  moieties could interact and give origin to an electrostatic complex. The search for a process involving cleavage of the O–Ge bond without attainment of complete separation of the resulting fragments allowed the determination of two transition structures (Figure 4a and b). These can be thought of as originating from the lithiated carbanion conformations: **4a** as originating from **1a–1b**, and **4b** from **1c**.

In transition structure **4a** ( $\nu_1 = 876.2i$   $\text{cm}^{-1}$ ) the transition vector is dominated by the following deformations (or their reverse). The motion of germyl away from O (0.53 coefficient) is coupled with the opening of the in-plane H'GeO angle (0.55 coefficient) and with some shortening of the CO bond ( $-0.34$  coefficient). The LiC distance (0.11 coefficient) and the LiCO angle ( $-0.21$  coefficient) are less important contributions. The energy barrier with respect to **1c** is more than twice as high as that for the direct Ge shift (Table 1), and this concerted dissociation appears to be most unlikely. For this reason the study of this structure was not extended to the CAS-MCSCF optimization. The second dissociation transition structure, **4b**, seemed more promising, on the basis of MP2 optimization. Due to the homolytic cleavage of the O–Ge bond, it was advisable to check the result at the more reliable CAS-MCSCF level. The MP2 and CAS-MCSCF levels are associated with basis sets that differ in the presence of diffuse functions, omitted in the latter

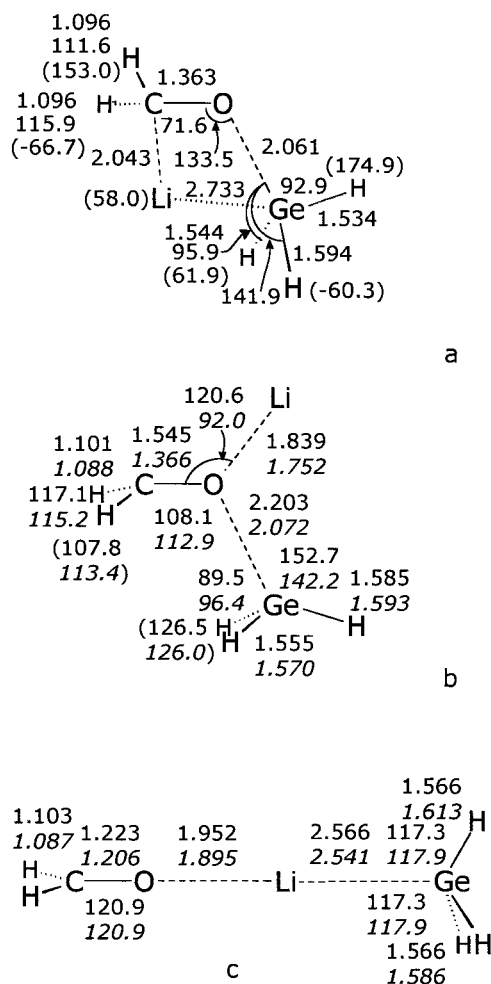


**Figure 4.** (a) Dissociation transition structure related to the gauche minimum. (b) Dissociation transition structure related to the W minimum, in which Li is antiperiplanar to Ge. (c) The electrostatic complex between a planar formaldehyde and germyllithium. Regular typeface: MP2 values. Italic: CAS-MCSCF values. Dihedral angles (in parentheses) defined as in Figure 1.

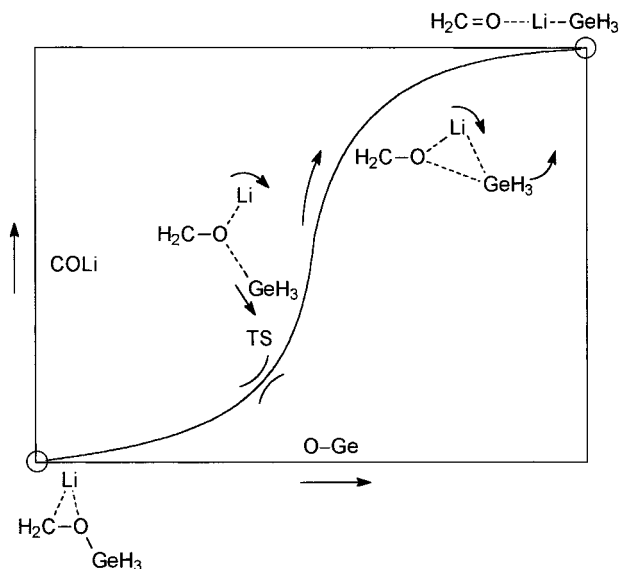
(see Methods section). To explore if diffuse functions are important in determining the TS geometry, an MP2 optimization without them was also carried out. All geometrical variations were modest (up to 0.04 Å and 3°), with the exception of the COLi angle, which is rather sensitive to the change of basis set and undergoes a closure from 120.6°, with diffuse functions, to 109.2°, without diffuse functions.

In the dissociation TS **4b** the cation participates by completely leaving the carbon atom and migrating to a position in which it interacts with both oxygen and germanium. The CAS-MCSCF vibrational analysis shows an imaginary frequency ( $\nu_1 = 792.0i$   $\text{cm}^{-1}$ ), in correspondence of which three main contributions appear in the Hessian eigenvector: the COLi angle (0.37 coefficient), the OGe distance (0.52 coefficient), and the in-plane HGeO angle (coefficient 0.61). These can be visualized as opening, elongation, and clockwise rotation, respectively (or the reverse). This attribute of the transition structure prompts us to further examine the corresponding pathway. An IRC analysis,<sup>11</sup> carried out at the CAS-MCSCF level in the vicinity of TS **4b**, confirms this interesting feature, showing that in correspondence to the TS elongated O–Ge bond length, the

**Table 2. Total<sup>a</sup> and Relative<sup>b</sup> Energies of the Additional Points (see Scheme 2)**

structure <sup>d</sup>	LiÖC	LiO	GeÖC	OGe	CCSD(T)/6-311+G(d) <sup>c</sup>		CAS-MCSCF/[542/341/21/2]	
					<i>E</i>	$\Delta E$	<i>E</i>	$\Delta E$
reactant <b>1a</b>	73	1.78	117	1.77	-2198.886329	0.0	-2196.334741	0.0
dissoc TS <b>4a</b>	92	1.75	113	2.07	-2198.847637	24.3	-2196.297032	23.7
	100	1.73	111	2.27	-2198.840736	28.6	-2196.302080	20.5
	110	1.72	112	2.27	-2198.839200	29.6	-2196.303630	19.5
	120	1.72	112	2.27	-2198.838921	29.7	-2196.305424	18.4
	130	1.71	114	2.27	-2198.840714	28.6	-2196.307740	16.9
	140	1.70	115	2.30	-2198.845153	25.8	-2196.310821	15.0
	142	1.70	115	2.31	-2198.846371	25.1	-2196.311583	14.5
	143	1.70	116	2.33	-2198.847082	24.6	-2196.312001	14.3
	145	1.91	135	4.40	-2198.901029	-9.2	-2196.399614	-40.7
complex <b>4c</b>	180	1.95	180	4.52	-2198.902820	-10.3	-2196.402405	-42.5
homolytic dissoc limit					-2198.815492	44.4 <sub>5</sub>	-2196.272534	39.0
heterolytic dissoc limit					-2198.873448	8.1	-2196.373482	-24.3

<sup>a</sup> Hartrees. <sup>b</sup> kcal mol<sup>-1</sup>, with respect to the initial lithiated carbanion **1a**. <sup>c</sup> Computed at the CAS-MCSCF/[542/321/21/2] geometries of the critical points. <sup>d</sup> Bond lengths in Å, angles in deg.

**Scheme 2**

more important deformations undergone by the dissociating molecule implicate a Li motion around O, with Ge getting closer to Li. This trait suggests a curved reaction pathway, such as that displayed in Scheme 2, leading toward the electrostatic complex.

In Figure 4c the optimized structure of such an electrostatic complex is shown. It is a rather stable structure (Table 1). From this energy minimum, reassociation of the two molecules could then take place to give the product. The IRC study has been flanked by a series of constrained CAS-MCSCF geometry optimizations that were performed in correspondence to various values of the COLi angle, to better define the above picture (Table 2). As the COLi angle gets close to 145°, the COGe angle opens further and the germyl group is “captured” by the cation, as sketched in Scheme 2. The system finally collapses to the complex minimum **4a**. Table 3 displays some data pertinent to this pathway. The abrupt modification in the CAS-MCSCF wave function nature occurring at a COLi angle value of 145° is notable and is illustrated in this table by the change in weight of the two more important electronic configurations.<sup>10b</sup> As germanium becomes tightly associated with the lithium cation, the wave function switches in nature from something between heterolytic and homolytic (that would be characterized by a single dominant configu-

**Table 3. Germyl Group Charges ( $Q_{\text{GeH}_3}$ )<sup>a</sup> and Highest CI Coefficients ( $c_i$ ) in the CAS-MCSCF Wave Function<sup>b,c</sup>**

structure	LiOC angle	$Q_{\text{GeH}_3}$		$c_1$	$c_2$
		NAO	(Mulliken)		
reactant <b>1a</b>	73	0.539	(0.429)	0.99	0.0
dissoc TS <b>4b</b>	92	0.042	(-0.047)	0.94	-0.30
	100	-0.166	(-0.226)	0.89	-0.43
	110	-0.187	(-0.248)	0.89	-0.43
	120	-0.210	(-0.272)	0.89	-0.43
	130	-0.239	(-0.303)	0.90	-0.42
	140	-0.295	(-0.359)	0.91	-0.40
	142	-0.318	(-0.381)	0.91	-0.39
	143	-0.341	(-0.402)	0.92	-0.37
	145d	-0.829	(-0.819)	0.97	-0.18
complex <b>4c</b>	179	-0.791	(-0.817)	0.98	-0.19

<sup>a</sup>  $Q_{\text{GeH}_3}$  charges are computed summing up Ge and H atomic NAO charges for the germyl group, within a natural bond orbital analysis (see ref 14); Mulliken group charges are also reported (in parentheses) for comparative purposes. <sup>b</sup> From CAS-MCSCF/[542/341/21/2] calculations defining the dissociation pathway of Scheme 2 and Table 2. <sup>c</sup> See note 10b. <sup>d</sup> At this value of the LiOC angle, germanium is “captured” by the lithium cation.

ration or two dominant configurations, respectively) to a clear heterolytic situation. This is further revealed by the charge modification on the germyl group as the geometry changes (Table 3). The group charges are obtained by summing up the atomic charges of the germyl group, computed as NAO charges within a natural bond orbital analysis.<sup>14</sup> For comparative purposes, the Mulliken group charges are also reported in Table 3. The coupled cluster energy profile (obtained by single-point energy evaluations in correspondence to the CAS-MCSCF geometries) has a maximum for a COLi angle larger than that of the CAS-MCSCF TS. Given that the diffuse functions are present only in the coupled cluster calculations, this can be an effect of the different basis sets, as discussed above. The lack of diffuse functions can also be the reason for the overemphasized stability of the complex and the heterolytic dissociation limit observed at the CAS-MCSCF level (Table 2). In **4c** the role of lithium in stabilizing the negative charge localized on germanium is probably overestimated; a similar effect operates on the formaldehyde plus germyllithium dissociation limit. It can be recalled, however, that the MCSCF calculations are not directed to an accurate assessment of the reaction energies.

Although dissociation through this pathway appears to be easier than that proceeding via **4a**, it is still difficult

(Table 1). In fact, this process requires overcoming a barrier ca. 13 kcal mol<sup>-1</sup> higher than that for the direct [1,2] Ge shift (compare the CCSD(T) results in Tables 1 and 2). In conclusion, both two-step processes beginning with cleavage of the O–Ge bond are unfavorable.

### Conclusions

The model reactions described in ref 3a (free anion) and in the present study (lithiated anion) correspond to two extreme situations of no interaction and tight interaction of the counterion with the anionic H<sub>2</sub>C–O–GeH<sub>3</sub> system. While the former case can be deemed to be pertinent to a gas-phase reaction, the mechanism in the condensed phase could be dependent to some extent on the degree of cation–anion interaction. In the lithiated system the direct germyl [1,2] migration is found to take place in a single kinetic step, passing through a cyclic transition structure, in which Ge is pentacoordinate. By contrast, in correspondence to this geometrical situation, the free anion exhibits an energy shoulder along a downhill pathway, that is preceded by a geometrically early transition structure associated with an energy barrier of only 2 kcal mol<sup>-1</sup>. These features of the energy profile for the direct [1,2] Ge shift are deeply modified in the lithiated system. Indeed, lithium stabilizes the cyclic structure less than the carbanionic reactant and the oxianionic product. As a consequence, it raises significantly the energy barrier, up to almost 17 kcal mol<sup>-1</sup>. The corresponding transition structure is thus later (in a geometrical sense) with respect to the free anion and shifts toward the cyclic arrangement that is typical, in the absence of a counterion, of the shoulder zone. The presence of Li<sup>+</sup> also reduces the reaction exothermicity, from 32 to 24 kcal mol<sup>-1</sup>. Notwithstanding these changes, the overall description of the mechanism provided by the two model systems is the same:

an exoergic one-step direct [1,2] migration of Ge from oxygen to carbon. In fact, also a dissociation/reassociation process can be envisaged, which could lead, by means of O–Ge bond cleavage, to an electrostatic complex between the formaldehyde, lithium, and germyl moieties. However, it comes out to be not favored in both the free and lithiated anion. In the former the relevant dissociation energy barrier is higher by 8 kcal mol<sup>-1</sup> than that for direct germyl migration, in the lithiated system by 13 kcal mol<sup>-1</sup>. Also in the case of the silicon Wright–West rearrangement, the energy barrier for dissociation had been found to be higher than that for silyl [1,2] migration, either in the absence or in the presence of Li<sup>+</sup>. The mechanism of both silicon and germanium rearrangements is thus described as a nondissociative shift of the silyl or germyl group. However, in the case of silicon the cyclic intermediate corresponds to a well-defined energy sag along the energy profile, and the reaction is a two-step one. Considering finally also the well-known Wittig rearrangement, the dissociative mechanism is described in that case as sharply preferred, but a mechanistic dichotomy is encountered. While a preference for O–C homolytic cleavage is found in the presence of Li<sup>+</sup>, the gas-phase reaction, modeled by the free anion system, is predicted to take place by a heterolytic mechanism.

In conclusion, it can be observed that these investigations have provided an assortment of distinct mechanisms for the rearrangements of simple model anionic and lithiated systems containing CH<sub>3</sub>, SiH<sub>3</sub>, and GeH<sub>3</sub> migrating groups.

**Acknowledgment.** This work has been supported by the Italian MURST.

OM990407G